

# MHONGOOSE commissioning observations of NGC 5068 using MeerKAT-64 and the narrow-band mode (April 2020)

Erwin de Blok<sup>1,2,3</sup>

<sup>1</sup> ASTRON, Netherlands Foundation for Radio Astronomy, Dwingeloo, Netherlands

<sup>2</sup> University of Cape Town, Cape Town, South Africa

<sup>3</sup> University of Groningen, Netherlands

version 05-08-2020

---

## Introduction

This report presents commissioning observations of the MHONGOOSE galaxy NGC 5068 (HIPASS J1318-21) using the narrow-band mode, which will be the main observing mode for MHONGOOSE. NGC 5068 was chosen as it was up during the night during the observing period in April. This galaxy is a more massive and extended galaxy than ESO 302-G014, the previous commissioning target.

The narrow-band mode has a bandwidth of 107 MHz and 32k channels, giving a channel width of 3.3 kHz or 0.7 km/s at 1.4 GHz. The HI velocity width of NGC 5068 is  $W_{20} = 111$  km/s, meaning we expect to see HI emission in something like ~150 individual channels.

The galaxy was observed for ~8 hours on April 28-29, 2020. Standard calibrator J1939-6342 was observed as the primary flux and bandpass calibrator, and J1311-2216 as the gain calibrator. Target and gain calibrator were observed sequentially, in a cycle of ~12 min on target, and ~2 min on the gain calibrator. The primary calibrator was observed twice during the observation, for a total of 20 mins.

Observation details are given below. The total observing times per source listed are prior to any flagging.

<i>Observation ID:</i>	20200428-0018
<i>Observing date/time (UTC):</i>	28-April-2020: 16:16—29-April-2020: 00:16 UTC
<i>Dishes:</i>	59 dishes (m023, m025, m036, m037, m043 not used)
<i>Target and observing time:</i>	NGC 5068: 355 minutes
<i>Primary calibrator and observing time:</i>	J1939-63: 20 minutes
<i>Secondary calibrator and observing time:</i>	J1311-22: 67 minutes

The data were obtained from the SARAO archive, where, prior to downloading, we extracted 1000 channels straddling 1417.0 MHz (the approximate central frequency of the galaxy). This 1000-channel data set was then downloaded directly to ASTRON in the Netherlands. The frequency range of this data set is 1415.36—1418.63 MHz.

The data were reduced at ASTRON with a pre-release version of the CARACa1 pipeline. This pipeline is an effort led by a team from SARAO and RATT and by the Fornax LSP team. More information on the pipeline is available at <https://caracal.readthedocs.io/en/>

latest. I am participating in this effort representing MHONGOOSE. A more extensive description of the pipeline is given in previous reports and is not repeated here.

---

## Data reduction

Initial inspection of the measurement set with `rfigui` showed clean data with only very minor RFI on a few baselines. We proceeded to flag the auto-correlations and any data suffering from shadowing. `AOFlagger` (within the pipeline) was then used to flag the calibrator data further based on the Stokes Q and U values. This involved a combination of sigma-clipping, filtering and extending existing flags. In the end all flagging steps described here resulted in  $\sim 16\%$  of the calibrator data being flagged (this number includes the auto-correlations).

Further inspection of the data showed residual RFI in the first five scans (16h16m-16h56m UTC). As the observed targets were still low above the horizon at that time, it is likely that ground RFI affected these data (shadowed dishes had already been flagged).

We derived the delay, bandpass and gain calibration solutions using the primary and secondary calibrators. Antenna m005 was found to have discrepant gain values which were not corrected in the calibration, and this antenna was flagged and the calibration redone.

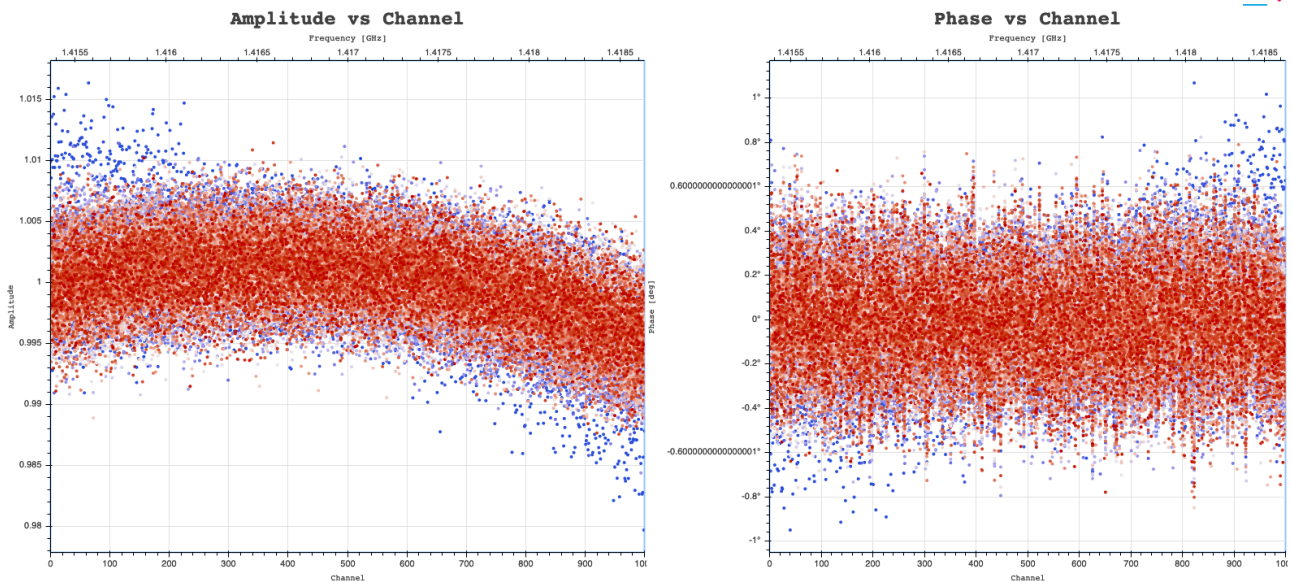


*Fig. 1. Amplitude (left) and phase (right) of the bandpasses of all antennas. Per channel the rms in the amplitude is  $\sim 0.25\%$  and  $\sim 0.12$  degrees in the phase. Blue points in the top-left of the amplitude panel are due to antenna m001. This antenna had slightly different solutions, which did, however, not affect the corrected data.*

The solutions were well-behaved. Figure 1 shows the bandpass amplitude and phase for all dishes. Bandpass amplitudes show a full range variation of  $\pm 0.5\%$ . Looking at the statistics per channel, the rms spread in the amplitudes is 0.25%. Only antenna m001 shows a slightly different behaviour which is, however, calibrated out. Phases also show only small scatter. The rms in a channel is 0.12 degrees.

The gain solutions also behaved satisfactorily. The flux of the secondary calibrator J1311-2216 was found to be  $5.265 \pm 0.003$  Jy at a frequency of 1417.0 MHz. For this calibrator, the VLA calibrator database lists a flux of 5.3 Jy at 20cm (no uncertainty given). Figure 2 shows the real and imaginary parts of the uv data for both primary and secondary calibrator, showing no systematic deviations from the expected behavior.

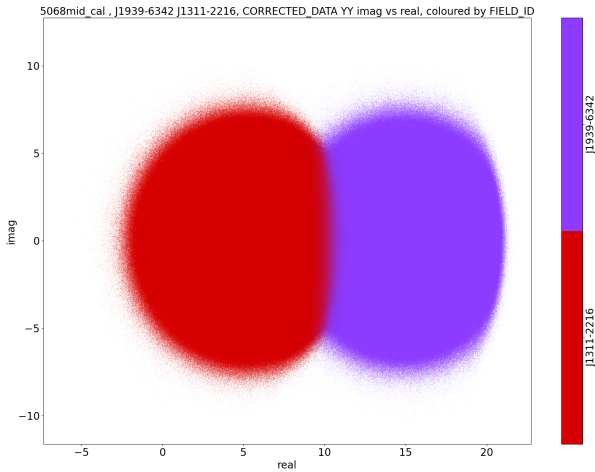


*Fig. 2. Real and imaginary parts of the visibilities of the primary (blue) and gain (red) calibrator.*

We applied these solutions to the target galaxy data, and split these off twice into two separate measurement sets. The first measurement set retained the original spectral resolution and was later used for the HI imaging. The second measurement set was produced by averaging by 250 channels in frequency, leading to a measurement set with 4 channels with a channel width of  $\sim 0.8$  MHz. This second measurement set was used for self-calibration. These data sets were also flagged with `AOFlagger`. In total (including scans close to the horizon, autocorrelations, RFI, shadowing),  $\sim 24\%$  of the target data were flagged.

We ran three self-calibration iterations, with the data subdivided in three equal frequency chunks. Solutions were derived for each of these chunks with a solution interval of 160 sec. For the three iterations, an increasingly deep automatic clean mask was defined at  $(20, 10, 5)\sigma$ . For the final image this limit was  $3\sigma$ . Sources in these masks were then cleaned to  $0.5\sigma$ . Images were created using robust weighting with a robust parameter equal to zero. We imaged a full  $2 \times 2$  degrees with a pixel size of  $2''$ . All chunks were then combined using a common synthesised beam of  $7.8'' \times 6.5''$ .

We measured the noise at several positions in the outer field of the final self-calibrated robust-weighted continuum image and found a value of  $33.1 \pm 0.7$   $\mu$ Jy/beam. To calculate the expected theoretical noise, we use the SEFD of MeerKAT in the 1415-1418 MHz frequency range as shown in Fig. 9 of the SARA0 “MeerKAT specifications” webpage<sup>1</sup> and use a value of  $395 \pm 1$  Jy. With the usual sensitivity equation we find a theoretical thermal noise of  $20.6$   $\mu$ Jy/beam. Using the ratio of 1.41 between robust=0.0 and natural-weighted noise found in previous commissioning observations, we find an expected noise in the continuum map of  $29.1$   $\mu$ Jy/beam. This is about 13% lower than our empirical noise, which is acceptable (and consistent with values found for previous commissioning observations). Most of this will be due to low-level uncleaned emission and faint sources.

The continuum image is shown in Fig. 3. Clearly visible in the centre is the complex and extended continuum emission of NGC 5068. The brightest source in the image has a peak flux of 42.1 mJy/beam, leading to a dynamic range (peak flux/noise) of 1270.

The self-calibration solutions were interpolated and applied to the measurement set with the original spectral resolution. The source list derived from the clean model of the final self-calibrated image was interpolated to the original spectral resolution and used to

<sup>1</sup> Available at <https://skafrica.atlassian.net/servicedesk/customer/portal/1/topic/bc9d6ad2-8321-4e13-a97a-d19d6d019a1c/article/277315585>

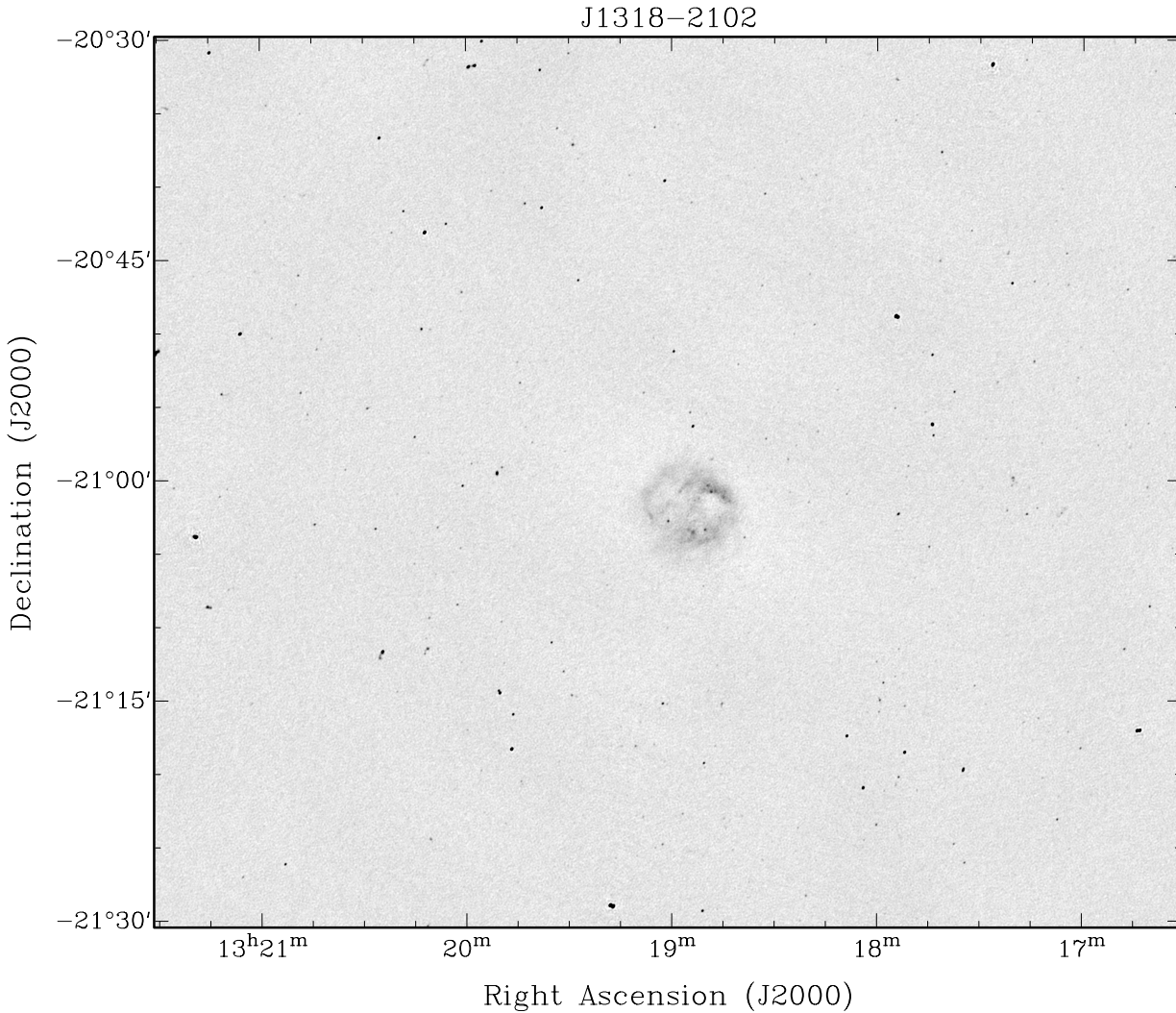


*Fig. 3. Continuum image of the 1 x 1 degree area surrounding NGC 5068. Image was created using a robust parameter of 0.0. The size of the beam is  $7.8'' \times 6.5''$ . The noise is  $33.1 \mu\text{Jy}/\text{beam}$ .*

construct a continuum model that was subtracted in the uv-plane from the target galaxy uv-data. This effectively removed all but the faintest continuum. An additional continuum subtraction step was then done by fitting the first and last 200 channels of the 1000 channel data in the uv plane with a linear function and subtracting the fit, resulting in a 600 channel data set containing only the HI emission.

---

## HI data reduction

We created image data cubes of 600 channels straddling the HI emission. These channels were deconvolved using `WSClean` in a two-step process. First a shallow ( $10\sigma$ ) clean mask was created automatically which was used to produce a preliminary deconvolved data cube. The source-finding program `SoFiA` was used on that cube to produce an improved clean mask which was applied in a second deconvolution to produce the final data cube. In principle, this could be repeated multiple times to further refine the mask. However, in this case using two iterations was found to be sufficient.

We produced a number of data cubes this way, using various values of the robustness parameter to explore the image quality and the HI morphology at various resolutions. The

Table 1: Properties HI data cubes

Robust value	Beam (arcsec)	Noise ( $\mu\text{Jy}/\text{beam}$ )	$N(\text{HI})$ ( $\text{cm}^{-2}$ ) $1\sigma$ , 1 channel	$N(\text{HI})$ ( $\text{cm}^{-2}$ ) $3\sigma$ , 16 km/s
0.0	8.1 x 6.7		973	$1.39 \times 10^{19}$
0.5	12.8 x 9.0		771	$5.21 \times 10^{18}$
1.0	25.3 x 17.4		660	$1.17 \times 10^{18}$
1.5	32.0 x 22.6		640	$9.88 \times 10^{17}$

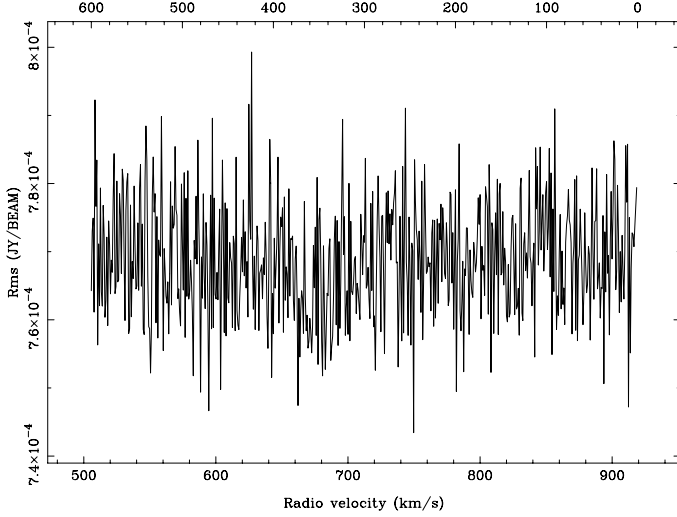
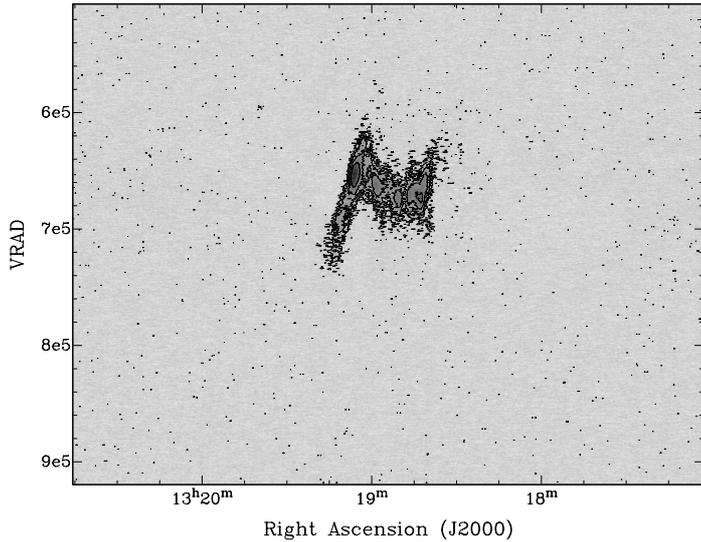


Fig. 4. Noise values in a line-free box in the  $r=0.5$  cube. Note the constancy of the noise over the entire velocity range.



$\text{robust}=1.5$  (close to natural-weighted) data set has a noise per channel of  $639.5 \pm 4.5 \mu\text{Jy}$  (as measured in a number of continuum-subtracted channel without HI emission). Using the same assumptions as above, we calculate an expected thermal noise of  $653.5 \mu\text{Jy}$  per 3.3 kHz channel. The measured noise is lower than the calculated noise, but this difference is only 2% and this can easily be attributed to the uncertainties in some of the assumptions (e.g., variation in the SEFD, variation of sensitivity with robustness parameter etc.). The noise levels in the HI data are thus close to the expected noise.

Table 1 lists the measured noise value for four values of the robust parameter, along with the corresponding beam size and the HI column density limit, both as a  $1\sigma$  limit in a single channel and as a  $3\sigma$  limit averaged over 16 km/s ( $\sim 23$  channels). The latter is a more useful value for comparing with sensitivities of observations in the literature that are usually obtained with a lower velocity resolution.

Figure 4 shows the noise in a line-free box in each channel as a function of velocity, showing that over the range considered here, the noise is stable and constant. Figure 5 shows a position-velocity slice along the RA axis crossing the target galaxy in the  $\text{robust}=1.0$  cube. The flatness of the background, the regular distribution of noise peaks and the lack of continuum subtraction

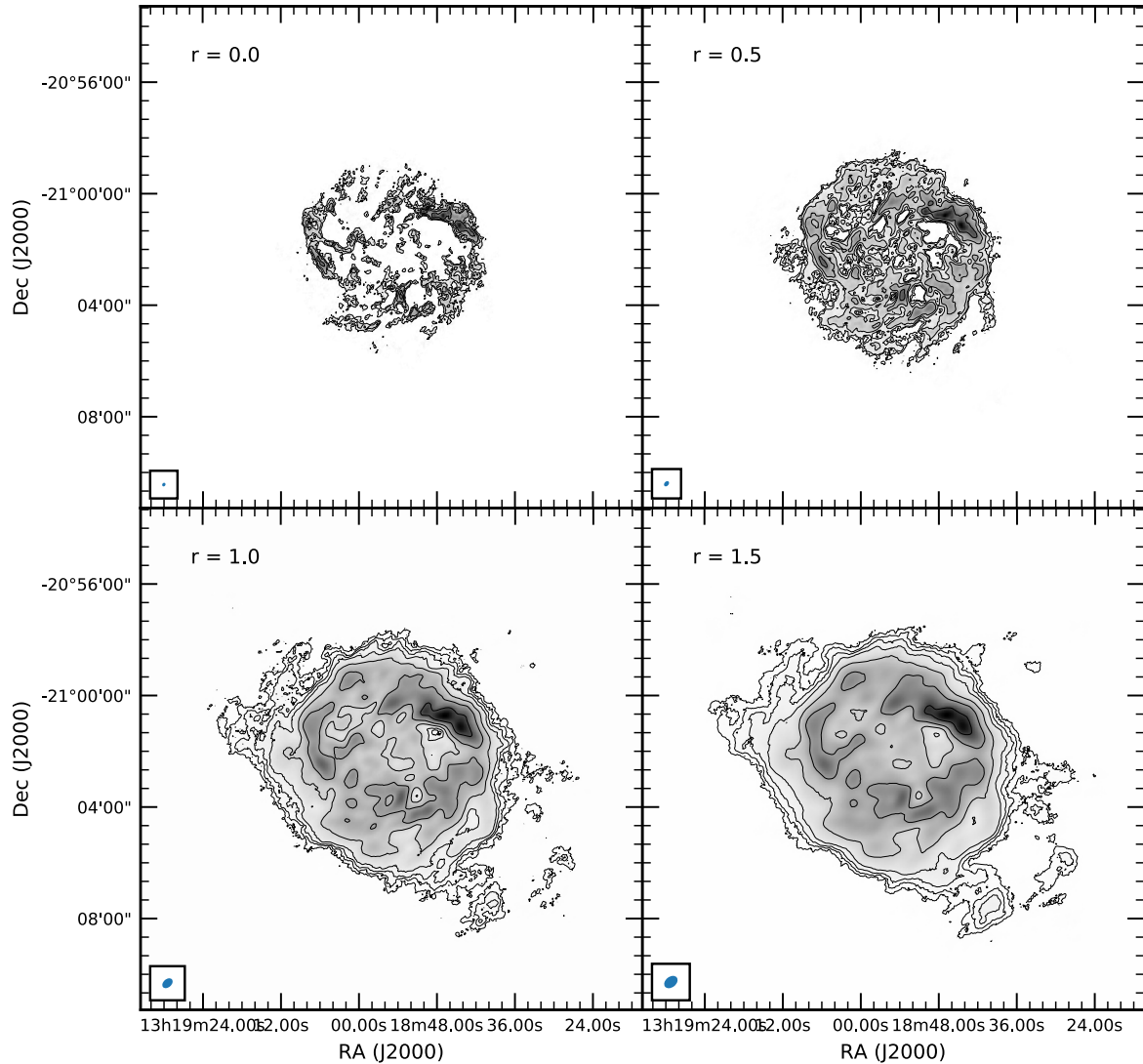


*Fig. 6. Integrated HI maps of galaxy NGC 5068 for  $robust=0.0, 0.5, 1.0, 1.5$  (from top-left to bottom-right) top row). The contour levels for each panel are as follows. Top-left:  $(2.0, 5.0, 10.0, 20.0) \cdot 10^{20} \text{ cm}^{-2}$ . Top-right:  $(1.0, 2, 5.0, 10.0, 20.0) \cdot 10^{20} \text{ cm}^{-2}$ . Bottom-left:  $(0.2, 0.5, 1.0, 2.0, 5.0, 10.0) \cdot 10^{20} \text{ cm}^{-2}$ . Bottom-right:  $(0.1, 0.2, 0.5, 1.0, 2.0, 5.0, 10.0, 20.0) \cdot 10^{20} \text{ cm}^{-2}$ . The beams are indicated in the lower-left corners.*

features all indicate good quality data.

Finally, for each of the four robust values, we produced an integrated HI intensity map (zeroth-moment map) by using a simple  $3\sigma$  selection criterion over the HI velocity range using the SoFiA source finding package with default reliability criteria. These moment maps are shown in Fig. 6. They show the familiar sequence of high-resolution, but limited column density to more limited resolution but better column density sensitivity.

---

## Summary

The HI observations presented here can be characterised as having an accurate, well-determined bandpass, a flat noise distribution as a function of frequency, accurately subtracted continuum, and good quality HI imaging. The narrow-band mode thus produces science-quality data in the frequency range imaged here.